International Research Journal of Pharmacy and Medical Sciences
ISSN (Online): 2581-3277

Coating of 3D Printed Scaffolds with PVA-Based Metallic Oxides Nanocomposites for Bone Tissue Regeneration

Raquel Couto de Azevedo Gonçalves Mota[1*], Emerson Oliveira da Silva[1], Lívia Rodrigues de Menezes[1]
[1]Instituto de Macromoléculas Professora Eloisa Mano. Universidade Federal do Rio de Janeiro. Rio de Janeiro. Brazil-21941-970
Email address: *raquel@nano.ufrj.br

Abstract— *Aiming to respond to the growing need for the development of a technology applied to bone tissue regeneration, polylactide (PLA) scaffolds were printed with a 3D fused filament printer that allows better control of the architecture and pore geometry. These scaffolds were coated with poly (vinyl alcohol) based nanocomposites and three different types of nanoparticles (zinc oxide, titanium oxide and zirconium oxide). The nanocomposites were obtained from a 7% PVA aqueous solution and a concentrario of 0,1% w/w of the nanoparticles. This nanocomposite was applied to the PLA scaffolds in order to increase the hydrophilicity of the scaffold and to generate bioactivity on its surface, since the added particles present osteoinduction capacity. After the coating, the scaffolds were characterized by NMR, TGA, DSC, SEM, compression tested, and had their biological activity measured by the evaluation of the deposition of hydroxyapatite on the surface of the scaffold. Based on the results, it can be determined that it is possible to coat the scaffold with the PVA matrix, and that these coatings can generate calcium and phosphate-based salt deposition activity on the surface. Moreover, the results indicated that the use of PVA based nanocomposites to coat scaffolds for application in bone regeneration is highly promising.*

Keywords— *Scaffold; 3D printing; Tissue Engineering; Bone Tissue; polymeric nanocomposites; metallic oxides.*

I. INTRODUCTION

Scaffolds are three-dimensional biocompatible structures that are able to mimic the properties of the extracellular matrix (ECM) of a given tissue, its mechanical support and bioactivity, which provides a platform for cellular adherence, proliferation and differentiation. For that reason, scaffolds are frequently used in tissue engineering to assist the regeneration of a damaged tissue, with a major application in bone regeneration [1–4].

The traditional methodology of scaffolds manufacturing includes techniques such as: solvent casting [5,6], porogen leaching [7], electrospinning [8] or a combination of all of these techniques [9]. Even though these techniques are largely applicable in the field, each has its own set of disadvantages, including: the use of toxic organic solvents, difficulty in removing residual solvent particles from the scaffold's matrix, long manufacturing period, low reproducibility of the techniques [10] and creating random and irregular pores due to lack of control of the architecture of the scaffold.

A great variety of studies show that the cell-material interaction plays an important part on tissue engineering, helping the cells migrate, proliferate and differentiate [11]. Therefore, the size, design and interconnectivity of the pores are essential factors that need to be considered when fabricating a scaffold [10]. Unlike the traditional scaffold fabrication techniques mentioned, 3D (three-dimensional) printing allows for more control of the scaffold's architecture, because the printed object is faithful to the computational model created. It allows for the construction of microstructures that mimic the porosity and the interconnectivity between the existing pores in the human body [12].

While revising the literature, it is possible to verify that polymeric matrices are widely used, due to their biocompatibility and especially their biodegradability, which constitutes of an important factor for the synthetic scaffold to be replaced by new tissue without leaving any residue [13]. In this aspect, PLA is particularly relevant because because it is already largely utilized in drug delivery and tissue engineering, and because, when it is biodegraded *in vivo*, it produces lactic acid, which is an intermediate substance in the natural metabolic cycle of carbohydrates in human organism [14].

One of the biggest problems researches face is to find a balance between its physical strength and it nutrient permeability, since these two parameters are inversely proportional; increasing the pore size increases the permeability to nutrient, but decreases the strength of the scaffold, and vice versa. However, the use of biodegradable polymers makes it possible to overcome this problem with the addiction of a inorganic phase, dispersed in the polymeric matrix, creating a composite or a nanocomposite stronger than the original scaffold, without having to compromise its nutrient permeability [15].

As it was said before, the osseointegration between the synthetic material and the bone tissue is of the most important criteria in the development of orthopedic implants. In that aspect, there are many studies that demonstrate that nanostructured materials promote protein interactions favorable to bone growth due to its surface properties. That happens because when a material is reduced to the nanometric scale there is a significant increase in the contact area, which

Raquel Couto de Azevedo Gonçalves Mota, Emerson Oliveira da Silva, and Lívia Rodrigues de Menezes, "Coating of 3D printed scaffolds with PVA-Based metallic oxides nanocomposites for bone tissue regeneration," *International Research Journal of Pharmacy and Medical Sciences (IRJPMS)*, Volume 2, Issue 2, pp. 55-62, 2019.

increases its physical-chemical properties, compared to those of the macrometric material [16].

Among the 3D printing techniques, fused deposition modelling stands out. In this technique, the material, in the form of a filament, is fused, extruded and deposited on a table, layer by layer. The material cools down, and it solidifies by itself, as it is extruded, so there is no need to use a light source or solvent, which could leave toxic residues in the structure of the scaffold [17]. The main limitation of this technique is the narrow range of materials that can be used, since only a few polymers have the thermal and rheological properties to be processed; PLA and the terpolymer acrylonitrile butadiene styrene (ABS) are the most commonly used [18].

In order to print nanostructured scaffolds it is necessary to go through and extra step and manufacture solid nanocomposite filaments for the printer to fuse and extrude, which increases the complexity and the cost of the process [18]. To avoid these complications, the authors have come with the idea of coating the fused filament scaffold with a layer of polymer nanocomposites. A good option for the coating is the use of Polyvinyl alcohol (PVA), a hydrophilic, non-toxic and biocompatible polymer. Due to its capacity of degrading in the body without leaving any toxic residue, this polymer is largely utilized in drug delivery systems.

PVA can present bioactivity with the addition of nanoparticles capable of osteoconductivity, such as hydroxyapatite, calcium phosphates, titanium dioxide [19], zinc oxide [20] and zirconium dioxide [21]. Coating hydrophobic PLA scaffolds with PVA matrices has the added advantage of reducing the recognition and immune reaction against them, as well as making the cellular adhesion process easier by making the surface of the material more hydrophilic [22].

The main objective of this paper will be to evaluate how the PVA-based nanocomposites coating will influence the thermal, chemical, mechanical properties and the bioactivity of the PLA scaffolds regarding their application in bone regeneration.

The nanoparticles chosen for this research were titanium oxide (TiO_2), zinc oxide (ZnO) and zirconium oxide (ZrO_2), since they are biocompatible.

II. Materials

For this paper, the following materials were used:

A. Polylactic acid, acquired in the form of filaments of RoHS-PLA 3D;
B. Polyvinyl alcohol, acquired from VETEC (Química Fina) with a hydrolysis level between 86,5% and 89,5%;
C. Titanium oxide acquired from Sigma Aldrich containing a particle size superior to 100 nm;
D. Zinc oxide acquired from Sigma Aldrich containing a particle size superior to 100nm;
E. Zirconium oxide acquired from Sigma Aldrich containing a particle size superior to 100nm.

III. Methodology

For the first step, the PVA nanocomposites were obtained through aqueous solution with one of the three different oxides used (zinc oxide, zirconium oxide and titanium dioxide) with the concentration of 0,1% w/w. For that effect, the 88% hydrolyzed PVA was solubilized in half of the water volume needed to obtain 7% w/w systems and kept in magnetic stirring for 1.5h at 80°C. After this stage, the solutions were left to rest for 24h.

After the 24h, the nanoparticles of each group were added to the other half of the deionized water and dispersed by introducing an ultrasound tip at 99% power for one minute, applying 3 intensity pulses every 15 seconds. Then the nanoparticles suspension were verted in the PVA solutions and they were kept stirring at room temperature for 1.5h.

Once the films of each group had been obtained, they were poured into plastic petri dishes and placed into an incubator at 60°C for 4 days to completely remove the solvent. These systems were analyzed in a previous work of the authors, proving that the nanoparticles were well dispersed in the polymeric matrix and increased the crystallinity of the nanocomposites [23].

Secondly, porous blocks designed to achieve a variable degree of porosity (between 30% and 50%) were printed in a fused filament printer, using a commercial PLA filament. The infill design chosen was the honeycomb, by the Slic3r tool, because this infill allowed us to achieve pore interconnectivity, which is necessary so there can be nutrient penetration and diffusion in a scaffold.

The scaffolds were printed in a KOIOS 3D printer with the following printing parameters: 4800 mm/min print head speed, filament feeding rate of 100 mm/min, extrusion temperature at 200°C and platform heat at 60°C.

These blocks were coated in the PVA nanocomposites solutions prepared in the first stage. After spending 4 days in the incubator at 60°C to dry, they were coated a second time to ensure the entire piece was coated. At the end of this process, these scaffolds were analyzed by the following techniques: differential scanning calorimetry (DSC), thermogravimetric analysis (TGA), Fourier transform infrared spectroscopy (FTIR), scanning electron microscope (SEM), mechanical compression tests and evaluation of calcium deposits after immersion in simulated body fluid.

IV. Characterization

Thermogravimetric analysis (TGA) was used to limit the analysis range of the DSC. TGA measurements were obtained with the TGA Q500 Thermogravimetric Analyzer (TA Instruments) in an interval from 40°C to 700°C and heating rate of 10°C/min under N_2 flow of 50mL/min.

The differential scanning calorimetry analysis (DSC) was used to determine the Glass transition temperatures of the scaffolds constituents (PLA and PVA) and melting point of PLA. This analysis was also important to define the crystallinity of these materials, since this parameter alters the scaffold's biodegradation. The analyses were run in TA-Instruments Q.1000 equipment under N_2 flow of 50mL/min, with heating rate of 5°C/min, between 0°C and 100°C. For these analysis, an analytic balance was used to measure out 10mg (± 0,2 mg) of each of the coated scaffolds.

Raquel Couto de Azevedo Gonçalves Mota, Emerson Oliveira da Silva, and Lívia Rodrigues de Menezes, "Coating of 3D printed scaffolds with PVA-Based metallic oxides nanocomposites for bone tissue regeneration," *International Research Journal of Pharmacy and Medical Sciences (IRJPMS)*, Volume 2, Issue 2, pp. 55-62, 2019.

They were only heated once, because after the first time, with the fusion of both materials, the systems would become a PLA and PVA mixture and lose their structure and conformation of the coating.

The crystallinity (X_c) of the pure scaffolds and the coated scaffolds was calculated with (1), by obtaining crystallization enthalpy (ΔH_c), heat of fusion (ΔH_f) and through heat of fusion of 100 % crystalline PLA, $\Delta H_{f100\%}$ = 94,0 J/g [24]. PLA was chosen for this analysis because it is the predominant compound in the scaffold, while the coating only represented 2% of the system, and for that reason, can be ignored in this analysis.

$$X_c(\%) = \frac{H_f - \sum Hc}{W_{PLA} x H_{f100\%}} x100 \quad (1)$$

In which: X_c (%) = degree of crystallinity; H_f = heat fusion of PLA in the sample, in J/g; $H_{f100\%}$ = heat fusion of hypothetically 100% crystalline PLA, in J/g; H_c = crystallization enthalpy of PLA in the sample, in J/g; W_{PLA} = PLA fraction in the sample obtained by the average of the TGA analysis, in %.

The enthalpy and temperature values were obtained with TA7000 software and the graphics were generated using the Origin 8.0 software.

The time-domain NMR analyses were achieved through the definition of longitudinal spin-lattice relaxation time (T_1H), measured with the inversion-recovery pulse sequence in the NMR Resonance Maran Ultra 0,54 T equipment for low field NMR. The samples were placed in an 18mm tube, which was placed in the probe. The frequency of the ^{1}H nuclei being observed was 23 MHz and the interval bandwidth of the waiting time between pulses p180x - τ - p90x and it varied between 0,01 – 10,000 ms with recycle interval of 3s.

The relaxometry analysis of the systems had the main goal of evaluating the molecular dynamics of thesystems obtained with the intention of establishing which of the systems had the best dispersion of nanoparticles in scaffold coating.

The samples were kept in contact with simulated body fluid at 37°C with the purpose of analyzing the calcium and phosphate deposition in their surfaces. After a period of 30 days in SBF, a sample was taken for analysis with the EDX technique to determine the existence and the quantity of said deposition.

Compression samples of coated and uncoated PLA scaffolds were investigated, to assess the influence of the coating and the porosity on the scaffolds. The samples (10x10x5mm) were 3D printed and coated with the nanocomposites, as described in the methodology. All samples were tested under axial compression by loading at a speed of 1 mm/s with a 5kN load. The compression modulus was calculated from the stress-strain curve as the slope of the initial linear portion of the curve. The compression modulus for any set of specimens were obtained by an average of three measurements.

The SEM analysis was conducted with the goal of identifying the printed scaffolds morphology before and after the PVA coating. For such, fragments of the scaffolds were attached to the surface of metallic stubs with the aid of a carbon tape, due to its adhesive and conductive surface. The stubs containing the samples were taken to BAL-TEC's Sputer Coater equipment, SDC 005 model, and covered with a layer of approximately 20nm of gold, to make the surfaces conductive, allowing for the capturing of images. The sample's images were obtained by using an Everhart-Thornley Detector (ETD) and a 25 kV.

V. Results and Discussion

The purpose of thie TGA analysis was to examine the influence of incorporating the nanocomposite coating into the PLA printed scaffold. In all samples, the curves showed only a degradation process, between 300°C and 400°C, very similar to the PLA degradation process described in the literature, and that is probably because PLA is the major component of the systems obtained. However, figure 1 show that the addition of the PVA coating has a negative impact on the thermal properties of the PLA scaffold. This behavior can be linked to the lesser thermal resistance of PVA, used in the coating of the scaffolds, which may have contributed to reduce the thermal resistance of the pure material (Table I).

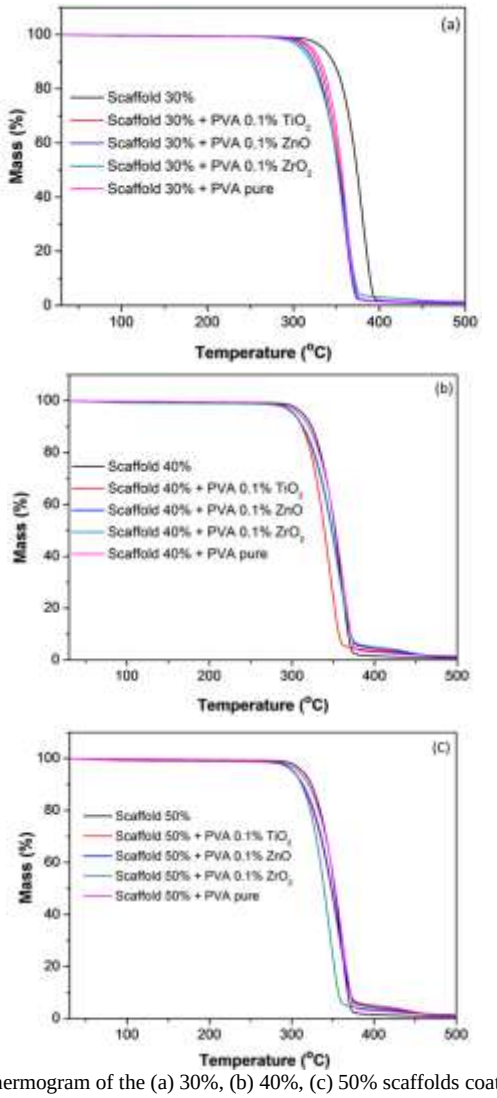

Fig. 1. Thermogram of the (a) 30%, (b) 40%, (c) 50% scaffolds coated with nanocomposites

Raquel Couto de Azevedo Gonçalves Mota, Emerson Oliveira da Silva, and Lívia Rodrigues de Menezes, "Coating of 3D printed scaffolds with PVA-Based metallic oxides nanocomposites for bone tissue regeneration," *International Research Journal of Pharmacy and Medical Sciences (IRJPMS)*, Volume 2, Issue 2, pp. 55-62, 2019.

International Research Journal of Pharmacy and Medical Sciences
ISSN (Online): 2581-3277

TABLE I. TGA Parameters of the scaffolds.

S. No.	TGA parameters		
	Sample name	T_{onset} (ºC)	T_{peak} (ºC)
1	Scaffold 30%	357	374
2	Scaffold 30% + PVA 0.1% TiO_2	341	361
3	Scaffold 30% + PVA 0.1% ZnO	339	360
4	Scaffold 30% + PVA 0.1% ZrO_2	327	356
5	Scaffold 40%	361	374
6	Scaffold 40% + PVA 0.1% TiO_2	345	363
7	Scaffold 40% + PVA 0.1% ZnO	342	359
8	Scaffold 40% + PVA 0.1% ZrO_2	343	359
9	Scaffold 50%	336	358
10	Scaffold 50% + PVA 0.1% TiO_2	322	349
11	Scaffold 50% + PVA 0.1% ZnO	321	347
12	Scaffold 50% + PVA 0.1% ZrO_2	323	346

The literature did not present any cases of other systems in the form of coated scaffolds so these results could be compared. Nevertheless, this result corroborates the research of Yeh *et al.*, (2008), which has produced PLA/PVA mixtures and evaluated their thermal resistances, testing through TGA pure PVA, pure PLA and the mixture of both polymers in various concentrations. The results demonstrate that the PVA's onset temperature is lower that pure PLA's, and has also determined that the decreasing order of thermal stability for the obtained systems was: PLA > PLA_{80}/PVA_{20} > PLA_{60}/PVA_{40} > PLA_{40}/PVA_{60} > PLA_{20}/PVA_{80} > PVA. Based in these results, it can be said that PVA's presence in the system compromises the thermal properties of the PLA/PVA mixture [25].

Based on the results with the pure scaffolds it can be said that the 50% porosity system showed inferior thermal resistance compared to the others (30% and 40% porosity). This behavior can be explained by the fact that thinner walls of the pores are printed from slimmer filament to make the scaffold more porous, as shown by the SEM analysis.

Comparing the thermal resistance of the scaffolds with the same porosity it is possible to see that there are no significant differences between the particles that were analyzed in any of the proposed systems. The cause of this can be the low concentration of the compounds, representing 0,1% of the coating's mass, that amounts to a small percentage of the scaffolds total mass. This way, its influence is probably ignorable regarding the thermal resistance of the systems.

The differential scanning calorimetry analysis (DSC) were run for both the coated and uncoated scaffolds to find out the values of their glass transition temperature (T_g), melting point (T_m) and to calculate their degree of crystallinity (X_c), to help determine how the coating process has influenced the thermal transitions in the obtained scaffolds. Considering that the system was mostly PLA, that was the scaffold's base, the thermal transitions relating to this polymer were the focus of the DSC analysis.As shown in to Table II, below, the T_gs of the 30% and 50% pure scaffolds were around the values stablished in the literature for PLA, which was T_g = 58ºC. The coated scaffolds had just one T_g, but with higher values, between 58°C and 79°C [26], meaning that their T_g was somewhere in between PLA's and PVA's T_g.

TABLE III. DSC Parameters of the scaffolds.

S. No.	DSC parameters					
	Sample name	T_g (ºC)	T_m (ºC)	ΔH_c (J/g)	ΔH_m (J/g)	Xc (%)
1	Scaffold 30%	58	169	22	29	18
2	Scaffold 30% + PVA 0.1% TiO_2	67	166	2	26	22
3	Scaffold 30% + PVA 0.1% ZnO	67	167	1	18	18
4	Scaffold 30% + PVA 0.1% ZrO_2	69	171	1	21	18
5	Scaffold 40%	69	167	20	25	18
6	Scaffold 40% + PVA 0.1% TiO_2	71	170	2	28	25
7	Scaffold 40% + PVA 0.1% ZnO	71	167	2	35	31
8	Scaffold 40% + PVA 0.1% ZrO_2	71	167	2	32	28
9	Scaffold 50%	56	170	25	34	20
10	Scaffold 50% + PVA 0.1% TiO_2	65	167	3	34	29
11	Scaffold 50% + PVA 0.1% ZnO	68	168	1	22	20
12	Scaffold 50% + PVA 0.1% ZrO_2	67	169	1	16	18

Abdal-Hay *et al.* (2015) have found similar results when creating PLA scaffolds through electrospinning, coated by PVA. They believe that the fact that there was only one T_g means there was a good interaction between PLA and PVA [27]. This means that the results of this paper can indicate that the polymers present good compatibility among themselves, providing a miscible system. However, it is important to note that the single T_g for all the systems can be a result of the low mass of PVA, which was below DSC's detection capacity.

The figure 2 (a, b and c) show that, after the T_g there is an exothermic peak and an endothermic peak, referring to the crystallization and the material's melting point, respectively. The melting point is around 166°C and 171°C for all samples, very similar values to those found in the literature for PLA's melting point (T_m) [28]. Thus, it is possible to state that the melting point observed was related to the PLA component of the system, while the PVA coating's melting point could not be observed in the chosen range.

The process of heating crystallization found in this study is common in polyesters like PLA, PHB and PCL, and shows how easy it is for these materials to crystallize, which makes them capable of generating a material's organization and crystallization as a response to the increase in mobility resulting from the heating of the system.

The crystallinity degree of the scaffolds is a very important parameter to calculate because the crystallinity is inversely related to its biodegradation, which is something of the utmost importance for this study since this event should occur at the same rate as bone tissue regeneration. So the crystallinity of the systems was calculated using equation 1, where $\Delta H_{m100\%}$ =

Raquel Couto de Azevedo Gonçalves Mota, Emerson Oliveira da Silva, and Lívia Rodrigues de Menezes, "Coating of 3D printed scaffolds with PVA-Based metallic oxides nanocomposites for bone tissue regeneration," *International Research Journal of Pharmacy and Medical Sciences (IRJPMS)*, Volume 2, Issue 2, pp. 55-62, 2019.

106J/m regarding PLA [29] and the results are shown in Table.

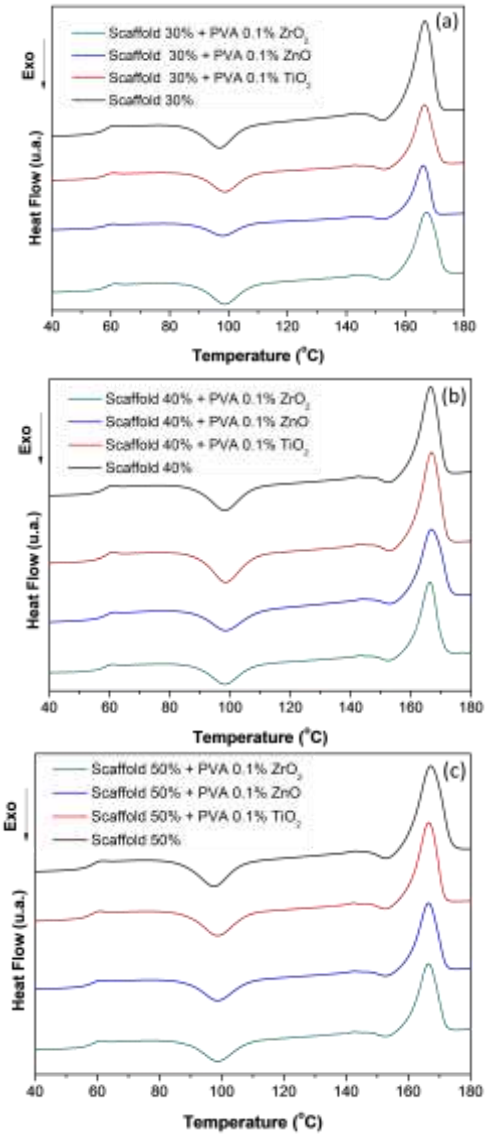

Fig. 2. DSC graphics of the (a) 30%, (b) 40%, (c) 50% scaffolds coated with nanocomposites

The coating of the scaffolds caused a significant alteration in crystallinity in some scaffolds and that can be explained by the process used to obtain these scaffolds. In order for the PVA coating to dry properly, the scaffolds were kept in an incubator at 80°C for 3 days, and each scaffold went through this process twice. As the coating's drying temperature was between PLA's T_g and T_m, this process probably caused an annealing, resulting on the observed increase in crystallinity.

TABLE IIIII. Spin-lattice relaxation times of the different porosity scaffolds

S. No.	NMR parameters	
	Sample name	T_1H (ms)
1	30% Scaffold	512
2	40% Scaffold	512
3	50% Scaffold	503

When the NMR results for the scaffolds with different porosity were compared, there was no difference in the T_1H time difference, in other words, porosity did not influence mollecular mobility of the polymeric chains (Table III).

This also applies when comparing scaffolds with different oxides (Table IV). There is no significant difference for any of the studied porosities, all the T_1H values were inside the margin of error of the equipment (5% of the value of the estimated time). This behavior indicated that the presence of the oxide did not alter the molecular mobility of the scaffolds, or that their low concentration, along with PVA's reduced mass in the system, could have limited the identification of its effect on the system just like it happened with TGA.

TABLE IVV. Spin-lattice relaxation times of the PVA coated scaffolds

S. No.	NMR parameters	
	Sample name	T_{onset} (°C)
1	30% Scaffold	512
2	30% Scaffold + PVA 0,1% TiO_2	525
3	30% Scaffold + PVA 0,1% ZnO	541
4	30% Scaffold + PVA 0,1% ZrO_2	532
5	40% Scaffold	512
6	40% Scaffold + PVA 0,1% TiO_2	524
7	40% Scaffold + PVA 0,1% ZnO	534
8	40% Scaffold + PVA 0,1% ZrO_2	526
9	50% Scaffold	503
10	50% Scaffold + PVA 0,1% TiO_2	523
11	50% Scaffold + PVA 0,1% ZnO	543
12	50% Scaffold + PVA 0,1% ZrO_2	530

Moreover, the scaffolds' bioactivity was evaluated through their immersion in SBF (simulated body fluid), a solution with ion concentrations that simulates the blood's plasma and is widely used to measure the subject's capacity to attract deposition of phosphate salts (Table V) like hydroxyapatite [30]. This trial is widely used as a mean to evaluate the osteoinducibility of the materials, considering their applications as bone scaffolds.

The addition of metallic oxides over the prosthetic structures or bone regeneration polymeric materials shows deposition activity of phosphate and calcium based salts in the human organism, especially in the form of hydroxyapatite. This behavior is possibly due to the presence of the PVA coating containing metallic oxides. In these systems both the nanoparticles and the polymeric matrix are rich in OH terminals, which present a partially negative charge. These charges tend to improve the deposition of said salts in the surface of the material.

The bioactivity regarding calcium deposition is extremely important for bone scaffolds because the deposition of calcium and phosphate based salts can represent the initial mechanism of osseointegration and works as a biological signal for osteoblasts and osteoclasts, which are responsible for repairing

Raquel Couto de Azevedo Gonçalves Mota, Emerson Oliveira da Silva, and Lívia Rodrigues de Menezes, "Coating of 3D printed scaffolds with PVA-Based metallic oxides nanocomposites for bone tissue regeneration," *International Research Journal of Pharmacy and Medical Sciences (IRJPMS)*, Volume 2, Issue 2, pp. 55-62, 2019.

the injured area. Based on the results it is observed that as the porosity of the scaffolds increases, there is an increase in their capacity for deposition of calcium and phosphate. This finding can be related to the better penetration of PVA coverage in these scaffolds due to the larger diameter of their pores.

TABLE V. Deposition of calcium and phosphate salts in the PVA/metallic oxides systems

S. No.	NMR parameters		
	Sample name	Ca (%)	P(%)
1	30% Scaffold (Without PVA coat)	0	0
2	30% Scaffold + pure PVA coating	1.1	0.6
3	30% Scaffold + PVA 0.1% TiO_2	12.6	5.6
4	30% Scaffold + PVA 0.1% ZnO	4,8	2,1
5	30% Scaffold + PVA 0.1% ZrO_2	7,6	3,5
6	40% Scaffold (Without PVA coat)	0	0
7	40% Scaffold + pure PVA coating	1.3	0.7
8	40% Scaffold + PVA 0.1% TiO_2	13.4	6.1
9	40% Scaffold + PVA 0.1% ZnO	5,1	2,3
10	40% Scaffold + PVA 0.1% ZrO_2	8,7	4,5
11	50% Scaffold (Without PVA coat)	0	0
12	50% Scaffold + pure PVA coating	1.9	1.2
13	50% Scaffold + PVA 0.1% TiO_2	18.1	8.7
14	50% Scaffold + PVA 0.1% ZnO	7.6	5.1
15	50% Scaffold + PVA 0.1% ZrO_2	12,8	7,6

Since scaffolds are intended to be used as bone substitutes, it is fundamental for them to achieve mechanical properties similar to that of natural bone. Cortical and cancellous bones have different mechanical strenghts because they have different pore volumes and sizes; the later has 75-85% porosity with 300-500 µm, while the former has 5-10% porosity with 10-50µm pore diameter. Therefore, cortical bone has a Young modulus of 90-230MPa, while cancellous's 2-45MPa [31,32].

Low mechanical strength is a major challenge in porous scaffolds, and is primarily controlled by its porosity, pore size and interconnectivity; for instance, the increase in the porosity is known to decrease exponentially the mechanical properties, which explains why the less porous scaffold (30%) has the higher modulus, followed by the scaffold with 40% porosity and finally the the one with the higher porosity (50%). Rodrigues et al. (2016) 3D printed scaffold using the FDM method with a porosity of 60% and, when mechanically tested, obtained a compression modulus around 200MPa, which is consistent with the results in this paper, shown in figure 3. They also tested a dense PLA scaffold and they noticed that by making the scaffold porous, the modulus descreases, going from 900MPa to 200 Mpa [33].

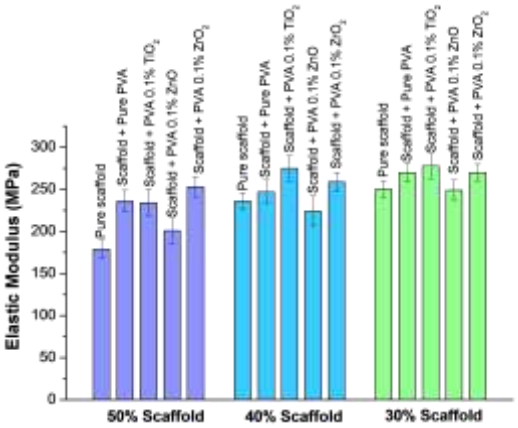

Fig. 3. Compressive elastic modulus of all tested groups

Comparing the uncoated scaffolds with different porosity degrees, it is easy to observe that the elastic modulus increases as the porosity decreases for the scaffolds becomes denser, like it was expected. According to the results, the coated scaffolds showed a better mechanical strength than the uncoated. This result is surprising because PVA is known to have worse mechanical properties than PLA, so the modulus was expected to decrease with the coating. However, the increase can be explained by the nanocomposites penetrating into the micropores, making the scaffold denser. This difference between coated and uncoated scaffold, however, is small, because during the coating method, the nanocomposites don't have time to penetrate the macropores and fulfill the entirety of the scaffold.

The zirconium and titanium coated scaffolds exhibit the best mechanical properties, while the zinc has the lowest of them all, and this is explained by the fact that the zinc oxide has a poor dispersion compared to the other metallic oxides, as shown in the NMR of a previous work. Overall, the results were satisfying, with a young modulus going from 150-300MPa, making the scaffolds suitable for bone tissue engineering.

Based on the results obtained, one can observe the porous pattern of the printed scaffolds (Figure 4, 5 and 6), as well as evaluate that its infill pattern corresponds to the honeycomb format, which is characterized by the use of hexagonal structures similar to those found in honeycombs.

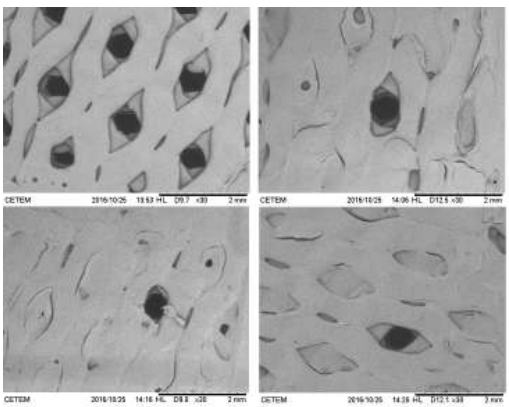
Fig. 4. MEV of scaffolds with 30% of porosity (a) without PVA coated; (b)PVA coatted 0.1% TiO_2; (c)PVA coatted 0.1% ZnO; (d)PVA coatted 0.1% ZrO_2;

Raquel Couto de Azevedo Gonçalves Mota, Emerson Oliveira da Silva, and Lívia Rodrigues de Menezes, "Coating of 3D printed scaffolds with PVA-Based metallic oxides nanocomposites for bone tissue regeneration," *International Research Journal of Pharmacy and Medical Sciences (IRJPMS)*, Volume 2, Issue 2, pp. 55-62, 2019.

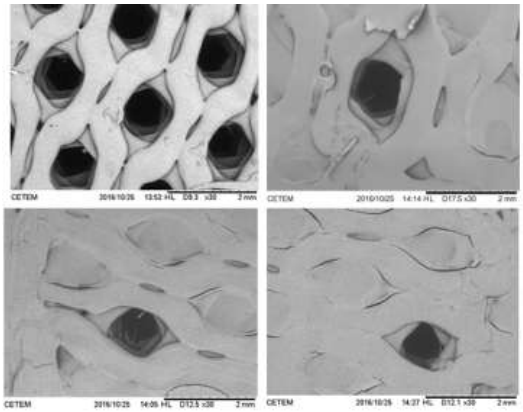

Fig. 5. MEV of scaffolds with 40% of porosity (a) without PVA coated; (b)PVA coatted 0.1% TiO_2; (c)PVA coatted 0.1% ZnO; (d)PVA coatted 0.1% ZrO_2;

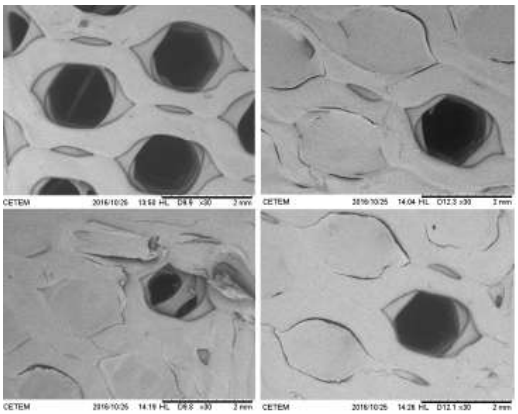

Fig. 6. MEV of scaffolds with 50% of porosity (a) without PVA coated; (b)PVA coatted 0.1% TiO_2; (c)PVA coatted 0.1% ZnO; (d)PVA coatted 0.1% ZrO_2

Among all the infill patterns that the modelling software offers, the honeycomb was chosen because it allows for a greater gain of mechanical resistance since it's a voronoi-like structure and, even though it is not a perfect three-dimentional voronoi, it is still more resistant than other infills that follow patterns with less resistance.

The Voronoi is a decomposition of space, a mathematical diagram formed by dots. The voronoi has the capacity to homogeneously distributing the mechanical energy throughout the structure of the whole piece, alleviating the tension of specific spots, and granting more resistance to the material's intrinsic resistance.

These hexagonal designs follow the concept of biomimetics, a field of science that appropriates structures found in nature and their designs to achieve specific characteristics. In honeycombs case, as the name states, the inspiration comes from the design of the honeycombs created by bees, but this design can also be found all over nature.

Another important factor that the SEM images show is the size of the pores. Based on the electromicrographies of each group, it is possible to observe that the pore size increases as the porosity increases (30%-50%). The measurement of the size of each of the pores was estimated using IMAGE J imaging software and can be found in the Table VI, shown below.

TABLE VI. Diameter of the pore x porosity of the scaffold

S. No.	porosity parameters	
	Porosity (%)	Diameter of the pore (mm)
1	50	1,54
2	40	1,06
3	30	0,58

The results found for the pore sizes are larger than those described in the literature, which determines that, to ensure a good cellular penetration and osteogenesis, the ideal size of a pore should be around 100-400 μm [13]. A recent study has researched the effect of pore sizes (100, 200, 350 and 500 μm) in a polypropylene-based scaffold. The results show optimal proliferation of MC3T3-E1 cells for the scaffolds with 200 μm and 350 μm pores, while the scaffolds with 500 μm pores could not sustain cells for over 7 days [34]. Another study has corroborated these results, emphasizing that pores of 500 μm or more are too big for cellular interaction [35].

Regarding the scaffolds after the PVA coating, one can observe that the scaffold's structures were coated with the hydrophilic matrix through the proposed method, for the coated scaffolds have most of their pores coated and appear to be more electron-dense than the pure scaffolds due to this coating. Besides that, even though it can be observed that most of the structure was coated, it can also be determined that the coating process was not homogeneous since it left some pores exposed. That probably happens due to the way this coating was embedded, through the immersion of the sample in a solution. It is also possible to see irregularities and flaws in the layers and that happens because the fused filament 3D-printing technique is not as precise as, for instance, stereolithography or selective laser sintering.

VI. CONCLUSIONS

Based on the results obtained it was possible to conclude:

- The coating of the scaffolds with the PVA generated a slight decrease in the thermal stability and also a tendency to increase crystallinity;
- The porosity of the systems showed an inversely proportional correlation to the mechanical property. In this sense, the system with the highest porosity value (50%) presented worse mechanical modulus;
- As regards the bone application of these systems, it is observed that the addition of the PVA coating was able to generate slight increases in the elastic modulus of the systems as well as the deposition of salts of calcium and phosphate on their surfaces. After coating the systems with 50% of porosity presented the mechanical properties statistically similar to the others systems;
- The systems obtained indicated that the use of PVA based nanocomposites to cover scaffolds for application in bone regeneration was highly promising.

ACKNOWLEDGEMENTS

This work was supported by the Brazilian funding institutions FAPERJ and CNPQ. We also acknowledge IMA/UFRJ for researching support and CETEM for MEV analysis.

REFERENCES

[1] J. Patterson, M.M. Martino, J.A. Hubbell, Biomimetic materials in tissue engineering, Mater. Today. 13 (2010) 14–22.
[2] J.F. Mano, R.A. Sousa, L.F. Boesel, N.M. Neves, R.L. Reis, Bioinert , biodegradable and injectable polymeric matrix composites for hard tissue replacement : state of the art and recent developments, Compos. Sci. Technol. 64 (2004) 789–817.
[3] F.P.W. Melchels, J. Feijen, D.W. Grijpma, A review on stereolithography and its applications in biomedical engineering, Biomaterials. 31 (2010) 6121–6130.
[4] T. Patrício, M. Domingos, A. Gloria, P. Bártolo, Characterisation of PCL and PCL / PLA scaffolds for tissue engineering, Procedia - Soc. Behav. Sci. 5 (2013) 110–114.
[5] R. Huang, X. Zhu, H. Tu, A. Wan, The crystallization behavior of porous poly(lactic acid) prepared by modified solvent casting/particulate leaching technique for potential use of tissue engineering scaffold, Mater. Lett. 136 (2014) 126–129.
[6] C. Del Gaudio, E. Ercolani, F. Nanni, A. Bianco, Assessment of poly(e{open}-caprolactone)/poly(3-hydroxybutyrate-co-3-hydroxyvalerate) blends processed by solvent casting and electrospinning, Mater. Sci. Eng. A. 528 (2011) 1764–1772.
[7] A. Salerno, M. Fernandez-Gutirrez, J. San Rom??n Del Barrio, C. Domingo, Bio-safe fabrication of PLA scaffolds for bone tissue engineering by combining phase separation, porogen leaching and scCO2 drying, J. Supercrit. Fluids. 97 (2015) 238–246.
[8] P. Wang, L. Zhao, J. Liu, M.D. Weir, X. Zhou, H.H.K. Xu, Bone tissue engineering via nanostructured calcium phosphate biomaterials and stem cells, Bone Res. 2 (2014) 14017–14030.
[9] C. Mendoza-buenrostro, H. Lara, C. Rodriguez, Hybrid fabrication of a 3D printed geometry embedded with PCL nanofibers for tissue engineering applications, Procedia Eng. 110 (2015) 128–134.
[10] K.F. Leong, C.M. Cheah, C.K. Chua, Solid freeform fabrication of three-dimensional scaffolds for engineering replacement tissues and organs, Biomaterials. 24 (2003) 2363–2378.
[11] M.N. Rahaman, D.E. Day, B. Sonny Bal, Q. Fu, S.B. Jung, L.F. Bonewald, A.P. Tomsia, Bioactive glass in tissue engineering, Acta Biomater. 7 (2011) 2355–2373.
[12] F. Pati, J.H. Shim, J.S. Lee, D.W. Cho, 3D printing of cell-laden constructs for heterogeneous tissue regeneration, Manuf. Lett. 1 (2013) 49–53.
[13] S. Bose, S. Vahabzadeh, A. Bandyopadhyay, Bone tissue engineering using 3D printing, Biochem. Pharmacol. 16 (2013) 496–504.
[14] A.K. Sutar, T. Maharana, S. Dutta, C.-T. Chen, C.-C. Lin, Ring-opening polymerization by lithium catalysts: an overview, Chem. Soc. Rev. 39 (2010) 1724–1746.
[15] C.-C. Yang, C.-T. Lin, Preparation of the PVA/TiO2 nanocomposite polymer menbranes by a sol-gel process for alkaline DMFC, ECS Trans. 6 (2008) 17–44.
[16] L. Zhang, T.J. Webster, Nanotechnology and nanomaterials : Promises for improved tissue regeneration, Nano Today. 4 (2009) 66–80.
[17] L. Shor, S. Güçeri, X. Wen, M. Gandhi, W. Sun, Fabrication of three-dimensional polycaprolactone/hydroxyapatite tissue scaffolds and osteoblast-scaffold interactions in vitro, Biomaterials. 28 (2007) 5291–5297.
[18] G. Postiglione, G. Natale, G. Griffini, M. Levi, S. Turri, Composites : Part A Conductive 3D microstructures by direct 3D printing of polymer / carbon nanotube nanocomposites via liquid deposition modeling, Compos. PART A. 76 (2015) 110–114.
[19] A.C.F.M. Costa, M.A. Vilar, H.L. Lira, R.H.G.A. Kiminami, L. Gama, U. Federal, D.C. Grande, C. Grande, S. Carlos, Síntese e caracterização de nanopartículas de TiO 2 (Synthesis and characterization of TiO 2 nanoparticles), Cerâmica. 52 (2006) 255–259.
[20] Y. Zhang, T. Nayak R., H. Hong, W. Cai, Biomedical Applications of Zinc Oxide Nanomaterials, Curr Mol Med. 13 (2014) 1633–1645.
[21] Y.T. Liu, T.M. Lee, T.S. Lui, Enhanced osteoblastic cell response on zirconia by bio-inspired surface modification, Colloids Surfaces B Biointerfaces. 106 (2013) 37–45.
[22] N.G. Patel, A. Kumar, V.N. Jayawardana, C.D. Woodworth, P.A. Yuya, Fabrication, nanomechanical characterization, and cytocompatibility of gold-reinforced chitosan bio-nanocomposites, Mater. Sci. Eng. C. 44 (2014) 336–344.
[23] R.C. de A.G. Mota, E. Oliveira, L. Menezes, Effect of the Addiction of Metal Oxide Nanoparticles on the Physical , Chemical and Thermal Properties of PVA Based Nanocomposites, Mater. Sci. Appl. 9 (2018) 473–488.
[24] G. Stoclet, R. Seguela, J. Lefebvre, Morphology , thermal behavior and mechanical properties of binary blends of compatible biosourced polymers : Polylactide / polyamide11, Polymer (Guildf). 52 (2011) 1417–1425.
[25] J. Yeh, M. Yang, C. Wu, X. Wu, C.-S. Wu, Study on the Crystallization Kinetic and Characterization of Poly (lactic acid) and Poly (vinyl alcohol) Blends, Polym. Plast. Technol. Eng. 47 (2008) 1289–1296.
[26] L. Xiao, B. Wang, G. Yang, M. Gauthier, Poly (Lactic Acid) -Based Biomaterials : Synthesis, Modification and Applications, Biomed. Sci. Eng. Technol. 11 (2006) 247–284.
[27] A. Abdal-hay, A. Salam, H. Makhlouf, P. Vanegas, A Novel Approach for Facile Synthesis of Biocompatible PVA-Coated PLA Nanofibers as Composite Membrane Scaffolds for Enhanced Osteoblast Proliferation, Elsevier Ltd., 2015.
[28] T. Elakkiya, R. Sheeja, K. Ramadhar, T.S. Natarajan, Biocompatibility Studies of Electrospun Nanofibrous Membrane of PLLA-PVA Blend, J. Appl. Polym. Sci. (2012) 1–7.
[29] C.M. Paranhos, B.G. Soares, R.N. Oliveira, L.A. Pessan, D.S. De Freitas, D. Windmo, Microstructural Evaluation of Poly (vinyl alcohol) -Based Hydrogels Obtained by Freezing-Thawing Technique : Thermal Analysis and Positron Annihilation, J. Appl. Polym. Sci. 105 (2007) 899–902.
[30] K. Tadashi, H. Takadama, How useful is SBF in predicting in vivo bone bioactivity?, Biomaterials. 27 (2006) 2907–2915.
[31] S.A. Goldstein, The Mechanical Dependence Properties Of Trabecular Bone : On Anatomic Location And, Biomechanics. 20 (1961) 1055–1061.
[32] G. Hannink, J.J.C. Arts, Bioresorbability, porosity and mechanical strength of bone substitutes : What is optimal for bone regeneration ?, Injury. 42 (2011) 22–25.
[33] N. Rodrigues, M. Benning, A.M. Ferreira, L. Dixon, K. Dalgarno, Manufacture and characterisation of porous PLA scaffolds, Procedia CIRP. 49 (2016) 33–38.
[34] J.W. Lee, G. Ahn, D.W. Cho, J.Y. Kim, Evaluating cell proliferation based on internal pore size and 3D scaffold architecture fabricated using solid freeform fabrication technology, J. Mater. Sci. Mater. Med. 21 (2010) 3195–3205.
[35] T.C. Lim, K.S. Chian, K.F. Leong, Cryogenic prototyping of chitosan scaffolds with controlled micro and macro architecture and their effect on in vivo neo-vascularization and cellular infiltration, J. Biomed. Mater. Res. - Part A. 94 (2010) 1303–1311.